AIDA – From airborne data inversion to in-depth analysis

Automatic detection and classification of induction anomalies in helicopter-borne electromagnetic data sets

Angelika Ullmann, Bernhard Siemon, Marion Miensopust

Federal Institute for Geosciences and Natural Resources, Germany

Introduction

Helicopter-borne electromagnetic (HEM) surveys reveal the spatial conductivity distribution in the subsurface, e.g., for groundwater or mineral exploration. Since the footprint of an HEM system is limited and smooth conductivity structures are close to 1-D settings 1-D inversion of HEM data is widely used. However, conductivity structures with strong lateral variations (induction anomalies) are not reproducible by standard 1-D inversion procedures and require multidimensional modeling. Thus, the information where such induction anomalies occur in an HEM data set is crucial. We present a new search algorithm for identification, selection, classification, and extraction of induction anomalies in HEM data sets. The search algorithm is tested on real HEM data, which were collected by a five frequency HEM system during a survey covering a buried valley. Due to the conductivity contrast between the clay layer in the buried valley and the surrounding material, the buried valley clearly appears on conductivity maps as a SSW-NNE running structure (Fig. 1). 3-D modeling is carried out for the identified anomalies.

Search algorithm

The measured secondary field data are transformed to the half-space parameter apparent resistivity ρ_a (Siemon, 2001). Then, 2-D grids of the logarithmic ρ_a are produced with a cell size of 50 m at four frequencies (Fig. 1). The search algorithm, consisting of several image processing methods (Canny, 1986; Sonka et al., 1993), is applied to grids of the absolute value of the horizontal gradients of ρ_a. Only areas with the strongest horizontal gradients are selected (Fig. 2) and the corresponding indicators are summed up to show anomalies at multiple frequencies (Fig. 3, left).

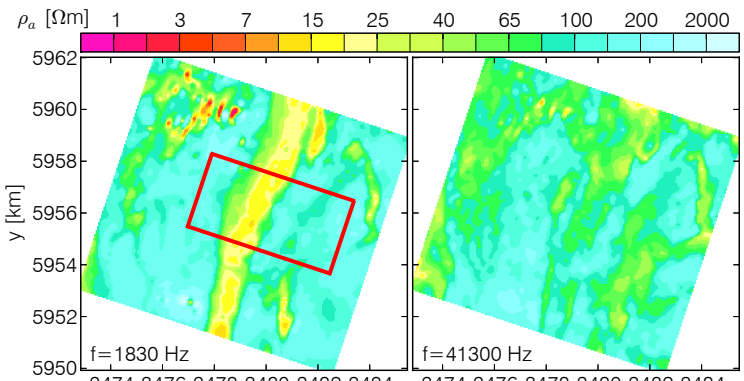

Fig. 1: Apparent resistivities at two frequencies. The red box marks the area where the 3-D modeling is carried out.

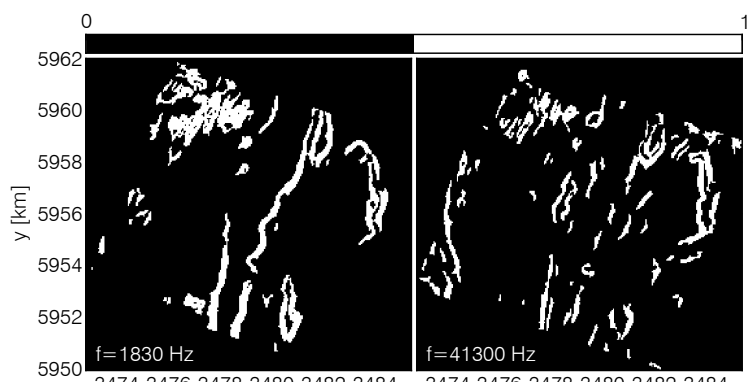

Fig. 2: Identified areas with the strongest horizontal gradients in two 2-D apparent resistivity grids.

Classification

A labeling algorithm (Sonka et al., 1993) is applied to the results of the search algorithm in order to identify connected anomalous areas (color-coded, Fig. 3, right). The detected induction anomalies are sorted in four different classes ("2-D", "3-D circular", "3-D oval", "3-D elongate"). The region-based shape descriptors compactness, eccentricity, and elongatedness (Sonka et al., 1993) are grouped to the corresponding classes by using the k-means algorithm (Lloyd, 1982) (Fig. 4, left). The induction anomalies are divided into 2-D and 3-D structures, in which the 3-D structures are differentiated into circular, oval, or elongated shapes (Fig. 4, right).

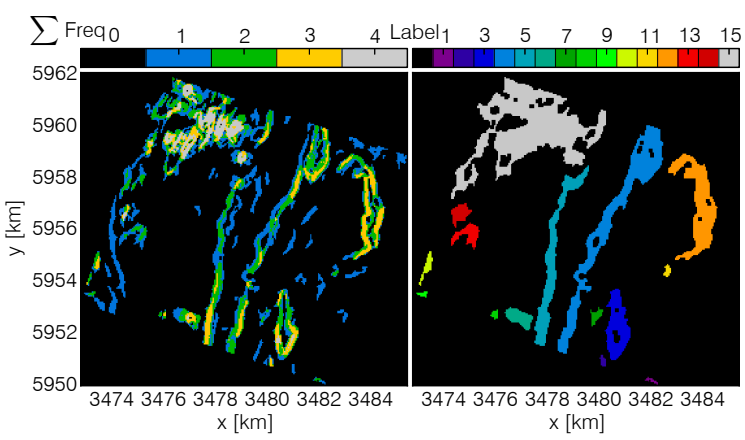

Fig. 3: Location and number of frequencies where induction anomalies were detected (left). Labeled detected induction anomalies (right).

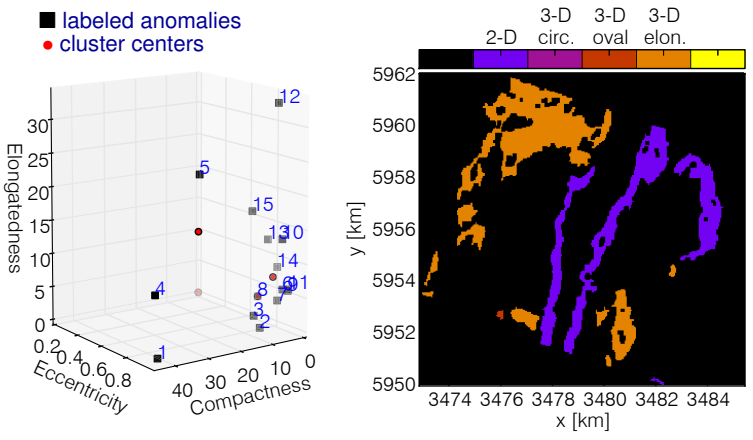

Fig. 4: Detected induction anomalies grouped into 2-D and 3-D structures (left). Classified detected induction anomalies (right).

Normal field transform

Before anomalous data can be extracted from the HEM data set, a certain area around the induction anomaly of interest is defined (cf. red box in Fig. 1). All detected anomalous regions within this area are enlarged about the size of two footprints (here 200 m) and masked out (Fig. 5, left). A 1-D background field Z_n can be calculated from the remaining averaged half-space parameters. A quasi 1-D field Z_{q1D}, valid for the 1-D host without anomalies, is derived from 2-D half-space parameter grids with anomaly gaps closed by gridding. The background field Z_n and the quasi 1-D field Z_{q1D} is used to transform the measured secondary field data Z according to $Z_{nft} = Z - Z_{q1D} + Z_n$ (Fig. 5, right). The resulting data can also be visualized by the half-space parameter ρ_a (Fig. 6).

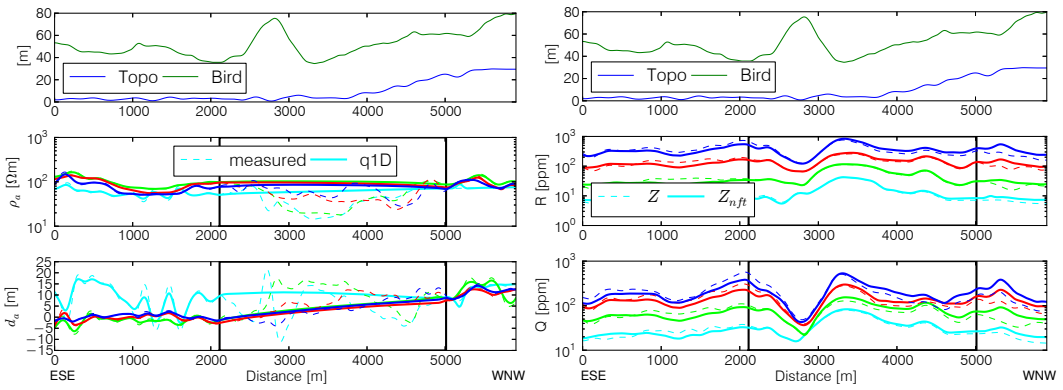

Fig. 5: On the left, original half-space parameters apparent resistivtiy ρ_a and apparent depth d_a derived from measured secondary field data (dashed line) and half-space parameters of the quasi 1-D host without anomaly derived from 2-D half-space parameter grids (solid line). On the right, measured secondary field data Z (dashed line) and transformed secondary field data Z_{nft} (solid line) shown as in-phase R and out-of-phase Q components, $Z = R + iQ$. The black lines indicate where the anomaly is cut out. The top panel shows the topography (blue line) and the sensor height (green line). The plotted data belonging to the four frequencies are color-coded: 384 Hz —, 1830 Hz —, 8610 Hz —, 41 300 Hz —.

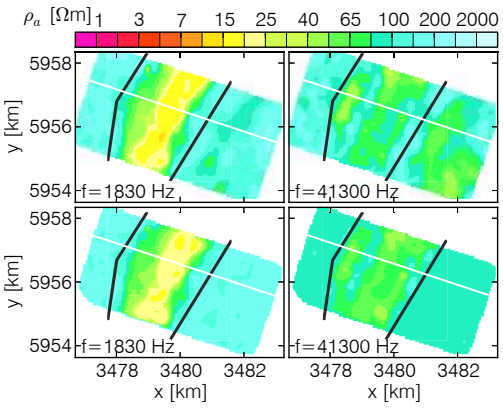

Fig. 6: Original apparent resistivity at two frequencies in the modeling area (upper panel). 1-D background model for the quasi 1-D host containing the buried valley pictured by two apparent resistivities (lower panel). The black lines indicate where the anomaly is cut out. The white lines show the location of the profile of interest.

3-D Modeling

A simplified model consisting of two conductive blocks in a 90 Ωm homogeneous half-space was chosen for a first synthetic test to fit the selected transformed secondary field data (Fig. 7). The integral equation code MarcoAir as part of the AMIRA project P223D (Raiche et al., 2007) was used for 3-D forward modeling. For detailed information on the forward modeling see the **poster** of **Miensopust et al.** "Three-dimensional modelling of frequency-domain helicopter-borne electromagnetic data: A case study of the Cuxhaven buried valley" at this conference.

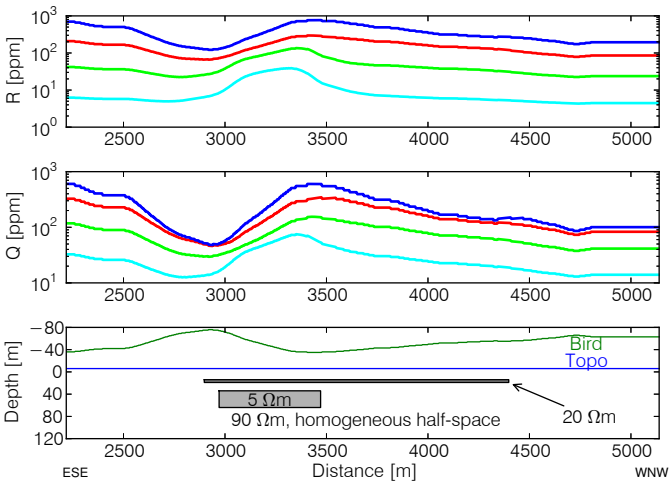

Fig. 7: In-phase (top panel) and out-of-phase (middle panel) values obtained for four frequencies using the model shown in the lower panel. The topography is set to a constant value. The measured sensor height is used but is rounded to integer meters. The plotted data belonging to the four frequencies are color-coded: 384 Hz —, 1830 Hz —, 8610 Hz —, 41 300 Hz —.

Conclusion

The newly developed search algorithm is able to automatically identify, select, classify, and extract induction anomalies in HEM data sets. The method is successfully tested on real HEM data covering a buried valley. The conductivity contrast between the sediments in the buried valley and the surrounding material induce induction anomalies on the edges of this geological body. They are detected and classified as 2-D structures by the search algorithm. The results are used to set up a simplified model for 3-D forward modeling of the buried valley.

Contact:

Angelika Ullmann

Email: angelika.ullmann@bgr.de

References:

Canny, J. (1986). A computational approach to edge detection. *IEEE Transactions on Pattern Analysis and Machine Intelligence*, *8*(6), 679–698.

Lloyd, S. P. (1982). Least Squares Quantization in PCM. *IEEE Transactions on Information Theory*, *28*(2), 129–137.

Raiche, A., Sugeng, F., & Wilson, G. (2007). Practical 3D EM inversion – the P223F software suite. *ASEG Extended Abstracts*, *2007*(1), 1–5.

Siemon, B. (2001). Improved and new resistivity-depth profiles for helicopter electromagnetic data. *Journal of Applied Geophysics*, *46*, 65–76.

Sonka, M., Hlavac, V., & Boyle, R. (1993). *Image Processing, Analysis and Machine Vision*. Chapman & Hall Computing.

Funded by:

Bundesministerium für Bildung und Forschung